Dressed Quark Mass Dependence of Pion and Kaon Form Factors

Y. Ninomiya,[1,*] W. Bentz,[1] and I. C. Cloët[2]

[1] *Department of Physics, School of Science, Tokai University, 4-1-1 Kitakaname, Hiratsuka-shi, Kanagawa 259-1292, Japan*

[2] *Physics Division, Argonne National Laboratory, Argonne, Illinois 60439, USA*

The structure of hadrons is described well by the Nambu–Jona-Lasinio (NJL) model, which is a chiral effective quark theory of QCD. In this work we explore the electromagnetic structure of the pion and kaon using the three-flavor NJL model in the proper-time regularization scheme, including effects of the pion cloud at the quark level. In the calculation there is only one free parameter, which we take as the dressed light quark (u and d) mass. In the regime where the dressed light quark mass is approximately 0.25 GeV, we find that the calculated values of the kaon decay constant, current quark masses, and quark condensates are consistent with experiment and QCD based analyses. We also investigate the dressed light quark mass dependence of the pion and kaon electromagnetic form factors, where comparison with empirical data and QCD predictions also favors a dressed light quark mass near 0.25 GeV.

PACS numbers: 12.39.Ki, 13.40.Gp, 14.40.Be, 14.40.Df

I. INTRODUCTION

Since the 1960s there have been substantial efforts, both experimental and theoretical, to unravel the quark structure of hadrons. The electromagnetic form factors of the various hadrons have played a crucial role in this process, as they reflect their internal quark (and gluon) structure [1–3]. The form factors of the pion and the kaon are of particular interest, because these mesons are associated with the Goldstone modes of dynamical chiral symmetry breaking [4] and play important roles in the description of the nuclear force [5]. The pion form factor has been measured in the region of low to medium momentum transfer [6, 7] and future measures at higher momentum are planned [8]. The kaon form factor, on the other hand, is poorly known experimentally, except in the region of very low momentum transfer [9]. On the theoretical side, QCD based studies of the pion and kaon form factors have been carried out, e.g., in the framework of perturbative QCD [10, 11], the Dyson-Schwinger equations [12–14] and the Nambu-Jona-Lasinio (NJL) model [15, 16].

The main purpose of this paper is to study the dressed (or equivalently constituent) quark mass dependence of the pion and kaon electromagnetic form factors, including effects from the virtual pion cloud around the dressed quarks and from vector mesons, using the three-flavor NJL model with four-fermion interactions. The NJL model is a powerful chiral effective quark theory of QCD [17, 18], with numerous successes in the study of meson [17, 19] and baryon [20–22] structure. In several recent studies [23–27] it has been demonstrated that one important aspect of quark confinement, namely, the absence of thresholds for the decay of hadrons into free quarks, can be implemented via a judicious choice for the regularization prescription. Following these lines, we will use the proper-time scheme [23, 28, 29] in this study. In our calculations there is only one free parameter, which we take as the dressed light quark (u and d) mass M.[1] The constituent quark model suggests dressed quark masses in the range $0.3-0.4$ GeV, and it is often fixed at 0.4 GeV in NJL model calculations of form factors [30, 31] and structure functions [24]. However, an important goal of our present study is to show that results for the current quarks masses, quark condensates, the kaon leptonic decay constant, as well as the pion and kaon charge radii and form factors, can be improved by using a smaller dressed light quark mass of $M \sim 0.25$ GeV. The dressed quark mass dependence of these observables is therefore investigated.

Recent experimental analyses of the current quark masses and pseudoscalar meson leptonic decay constants have found: $m_s/m = 27.5 \pm 1.0$ [32] and $f_K/f_\pi = 1.197 \pm 0.002 \pm 0.006 \pm 0.001$ [32, 33]. The lattice QCD calculations of Refs. [34, 35], which are extrapolated to the continuum limit, find $m_s/m = 27.53 \pm 0.20 \pm 0.08$ and for the pseudoscalar decay constants Refs. [36, 37] obtain $f_K/f_\pi = 1.1916 \pm 0.0021$. Both these results are in excellent agreement with experiment. Concerning quark condensates, a recent lattice QCD analysis [38] found $\langle \bar{s}s \rangle / \langle \bar{\ell}\ell \rangle = 1.08 \pm 0.16$ for the ratio of strange to light ($\ell = u, d$) nonperturbative (physical) quark condensates. As we shall see, our results for those three ratios m_s/m, f_K/f_π and $\langle \bar{s}s \rangle / \langle \bar{\ell}\ell \rangle$, together with the pion charge radius, are in excellent agreement with the empirical and QCD based results if the mass of the dressed light quark is approximately $M \sim 0.25$ GeV. We emphasize that, because our model is free of unphysical decay thresholds, there are no problems in obtaining hadron masses which are greater than the sum of their dressed quark masses,

* Corresponding author: 3bsnm017@mail.tokai-u.jp

[1] We assume isospin symmetry and denote $M_u = M_d = M$ for the dressed u and d quark masses, and $m_u = m_d = m$ for the associated current quark masses.

which is important for the extension of these studies to, e.g., the ρ meson and the nucleon. The main point which we wish to make in this paper is to show that the results for the pion and kaon form factors, as well as the other physical quantities mentioned above, can be much improved by using a rather small value of the dressed light quark mass. Corrections from the pion cloud and vector mesons to the quark-photon vertex are important to attain this good overall picture. In order to keep the simplicity of the NJL model description, however, we do not intend to present a full study of meson loops in this work. We will explicitly consider the meson loop corrections only for those processes which involve an external virtual photon probe, that is, the pion cloud corrections (see Fig. 6) and the corrections from ρ and ω mesons (see Fig. 8) to the quark-photon vertex. For the other processes, like those shown in Figs. 1, 2, 3, and 4 only that part of the pion loop effects which can be incorporated into the mass and wave function renormalization of the dressed quarks will be considered, which is sufficient to uphold various important low energy theorems (see App. C). This is essentially the same kind of approximation which has been implicitly used in numerous works on meson cloud and meson exchange current effects in hadronic [31, 39, 40] and nuclear [41, 42] physics. Nevertheless, a more complete study of meson loops, including their effects also on processes without an external probe [43, 44], should be an important goal for future studies.

The outline of this paper is as follows: In Sect. II we introduce the model and provide expressions that give the current quark masses, the masses of pion and kaon, and their leptonic decay constants. In Sect. III we calculate the pion and kaon form factors, and Sect. IV presents these results. A summary is given in Sect. V.

II. THE NJL MODEL

The NJL model [45, 46] is a successful chiral effective quark theory of QCD, that has been used to describe low to medium energy phenomena, such as dynamical chiral symmetry breaking and the associated dynamical quark mass generation. In this section we briefly explain the three-flavor NJL model with four-fermion interactions, together with the proper-time regularization scheme which avoids unphysical decay thresholds. We also illustrate the relation between the dressed and current quark masses, and discuss mesons as relativistic bound states of a dressed quark and anti-quark.

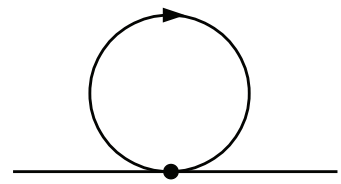

Figure 1. Quark self-energy in the mean-field approximation. The solid line represents a dressed quark propagator.

A. NJL Lagrangian and the Gap Equation

The three-flavor NJL model Lagrangian, with four-fermion interactions, reads

$$\mathcal{L}_{NJL} = \bar{\psi}(i\partial\!\!\!/ - \hat{m})\psi + G_\pi \left[(\bar{\psi}\,\lambda_a\,\psi)^2 - (\bar{\psi}\,\lambda_a\,\gamma_5\,\psi)^2\right] - G_v \left[(\bar{\psi}\,\lambda_a\,\gamma^\mu\,\psi)^2 + (\bar{\psi}\,\lambda_a\,\lambda_a\gamma_5\,\psi)^2\right], \quad (1)$$

where the quark field ψ has the flavor components $\psi = (u, d, s)$ and $\hat{m}$ denotes the current quark mass matrix $\hat{m} = \mathrm{diag}(m, m, m_s)$. A sum over $a = 0, \ldots, 8$ is implied in Eq. (1), where $\lambda_1, \ldots, \lambda_8$ are the Gell-Mann matrices in flavor space and $\lambda_0 \equiv \sqrt{\frac{2}{3}}\,\mathbb{1}$. To explicitly break the global $U_A(1)$ symmetry of Eq. (1) and describe, for example, also the η and η' mesons, a six-fermion (determinant) interaction [47] is often included in Eq. (1). However, because this term will not directly affect our main results on pion and kaon properties, we do not include it here for simplicity.[2] The four-fermion interaction term proportional to the coupling constant G_π in Eq. (1) describes the direct terms of the $\bar{q}q$ interaction in the scalar and pseudoscalar meson channels. This term is responsible for, *inter alia*, the dynamical breaking of chiral symmetry and consequentially the generation of dressed quark masses. The term proportional to G_v in Eq. (1) describes the direct piece of the $\bar{q}q$ interaction in the vector and axialvector meson channels.[3] The NJL model does not *a priori* contain quark confinement. However, one important aspect of quark confinement can be incorporated into the NJL model by introducing an infrared cut-off in the proper-time regularization scheme [23, 28, 29, 49]. This additional cut-off eliminates unphysical thresholds for the decay of hadrons into quarks, and at the same time respects all symmetry constraints. (Details of this regularization method are discussed further in App. A.)

[2] As pointed out in Ref. [48], in order to avoid an unstable vacuum, the inclusion of the six-fermion interaction makes it necessary to also include an eight-fermion interaction. In order to retain the simplicity of the model, we do not include these interactions in this work.

[3] In principle the flavor singlet and octet pieces of the G_v term in Eq. (1) can appear in the NJL interaction Lagrangian with separate coupling constants, as they are individually chirally symmetric. Our choice of identical coupling constants avoids flavor mixing, giving the ω meson as $(u\bar{u} + d\bar{d})$ and the ϕ meson as $s\bar{s}$.

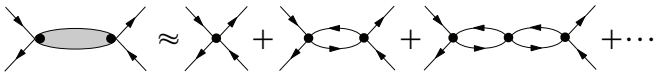

Figure 2. Random phase approximation for the quark-antiquark T-matrix.

In the mean-field approximation the dressed quark masses (M and M_s) are given by the quark self-energy illustrated in Fig. 1. Because the relevant interaction term in the NJL Lagrangian (Eq. (1)) is given by

$$G_\pi \sum_{a=0,3,8} \left(\bar\psi\lambda_a\psi\right)^2 = 2G_\pi \left[(\bar u u)^2 + \left(\bar d d\right)^2 + (\bar s s)^2\right], \quad (2)$$

the gap equations decouple in flavor space and take the familiar forms

$$\begin{aligned} M_q &= m_q - 4\,G_\pi\,\langle\bar q q\rangle \\ &= m_q + 48i\,G_\pi\,M_q \int \frac{d^4k}{(2\pi)^4}\,\frac{1}{k^2 - M_q^2 + i\epsilon}\,, \end{aligned} \quad (3)$$

where $q = u,\, d,\, s$, and $\langle\bar q q\rangle$ is the quark condensate. Using a Wick rotation and introducing the proper-time regularization gives

$$\frac{m_q}{M_q} = 1 - \frac{3\,G_\pi}{\pi^2}\int_{1/\Lambda_{UV}^2}^{1/\Lambda_{IR}^2} d\tau\;\frac{e^{-\tau M_q^2}}{\tau^2}. \quad (4)$$

The dressed quark propagators for the light and strange quarks are therefore given respectively by

$$S_\ell(p) = \frac{\not p + M}{[p^2 - M^2 + i\varepsilon]}, \quad (5)$$

$$S_s(p) = \frac{\not p + M_s}{[p^2 - M_s^2 + i\varepsilon]}, \quad (6)$$

and in flavor space the quark propagator has the form

$$S(p) = \mathrm{diag}\left[S_\ell(p),\, S_\ell(p),\, S_s(p)\right]. \quad (7)$$

B. Mesons and their couplings to quarks

The pion and kaon T-matrices are obtained by considering quark–antiquark scattering in the pseudoscalar channel using the random phase approximation (RPA), which is equivalent to the ladder approximation, and is illustrated in Fig. 2. Summing the bubble diagrams in Fig. 2 gives

$$T_k = \gamma_5\lambda_\alpha\,\frac{-2i\,G_\pi}{1 + 2\,G_\pi\,\Pi_k(p^2)}\,\gamma_5\lambda_\alpha, \quad (8)$$

where $k = \pi, K$; the sum over α takes the values $\alpha = 1,2,3$ for the pion ($k = \pi$) and $\alpha = 4,5,6,7$ for the kaon ($k = K$). The matrices $\gamma_5\lambda_\alpha$ act on the external quarks, and $\Pi_k(p^2)$ is the bubble diagram (polarization propagator) in the pion and kaon channels, illustrated in Fig. 3. These bubble diagrams take the form

$$\Pi_\pi(p^2)\,\delta_{\alpha\beta} = i\int\frac{d^4k}{(2\pi)^4}\;\mathrm{Tr}\left[\gamma_5\,\lambda_\alpha\,S_\ell(p+k)\,\gamma_5\,\lambda_\beta\,S_\ell(k)\right], \quad (9)$$

$$\Pi_K(p^2)\,\delta_{\alpha\beta} = i\int\frac{d^4k}{(2\pi)^4}\;\mathrm{Tr}\left[\gamma_5\,\lambda_\alpha\,S_\ell(p+k)\,\gamma_5\,\lambda_\beta\,S_s(k)\right], \quad (10)$$

where for the pion $\alpha,\beta = 1,\,2,\,3$ and for the kaon $\alpha,\beta = 4,\,5,\,6,\,7$. The trace is taken in Dirac, flavor and color space. Explicit forms for these bubble diagrams, in the proper-time regularization scheme, are given in App. B.

The pion and kaon masses, m_k, are defined by the pole in the corresponding T-matrix, therefore the pole conditions take the form

$$1 + 2\,G_\pi\,\Pi_k\big(p^2 = m_k^2\big) = 0, \quad \text{where} \quad k = \pi,\,K. \quad (11)$$

Near a bound state pole the T-matrix behaves as

$$T_M \sim \gamma_5\lambda_\alpha\,\frac{ig_k^2}{p^2 - m_k^2 + i\epsilon}\,\gamma_5\lambda_\alpha, \quad (12)$$

where g_k is identified as the quark–meson coupling constant. To derive expressions for g_k we expand Eq. (8) about the pole at $p^2 = m_k^2$. Using

$$\Pi_k(p^2) = \Pi_k(m_k^2) + \left.\frac{\partial\Pi_k(p^2)}{\partial\,p^2}\right|_{p^2=m_k^2}(p^2 - m_k^2) + \ldots, \quad (13)$$

gives

$$g_k^2 = -\left[\left.\frac{\partial\Pi_k(p^2)}{\partial p^2}\right|_{p^2=m_k^2}\right]^{-1}. \quad (14)$$

From the pole behavior in Eq. (12) we see that the quark-antiquark interactions are mediated by pseudoscalar particles. Hence, we can interpret m_k as the meson mass and g_k as the coupling constant of the meson to the quarks. We will use the pole approximation for the T-matrix, expressed by Eq. (12), throughout this work in order to keep meson loop integrals tractable analytically. The simple ladder approximation used here leads to pseudoscalar (γ_5) couplings of the pion or kaon to the quarks. It is well known [50] that also a mixing between the pseudoscalar and pseudovector interaction terms of the Lagrangian (1) can contribute to the T-matrix in the pseudoscalar channel, which leads to a pseudovector contribution ($\not p\gamma_5$) to the meson–quark coupling. Because this mixing is physically associated with the contribution of a heavy meson (the a_1 meson for the light flavor case) in the intermediate states, we neglect it here so as to keep the simplicity of the model description [4].

[4] For the case of the T-matrix in the pion channel, those mixing

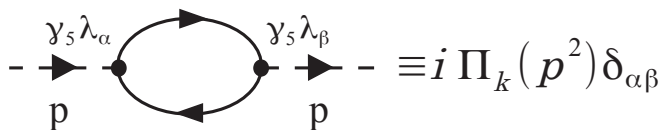

Figure 3. The pseudoscalar meson bubble diagram, $\Pi_k(p^2)$, where $k = \pi$, K. The dashed line represents a pion ($\alpha, \beta = 1, 2, 3$) or a kaon ($\alpha, \beta = 4, 5, 6, 7$).

C. Meson decay constants

The pion and kaon leptonic decay constants can be determined from the meson to hadronic vacuum matrix element, $\langle 0|j_a^\mu(0)|k_b(p)\rangle$ ($k = \pi,\ K$), where $j_a^\mu(x)$ is the weak axialvector current operator for flavor quantum number a. This matrix element is illustrated diagrammatically in Fig. 4, and therefore the pion and kaon leptonic decay constants, f_k, are defined by

$$\langle 0|j_a^\mu(0)|k_b(p)\rangle \equiv i\, p^\mu\, f_k\, \delta_{ab}. \tag{15}$$

The diagram in Fig. 4 gives, for the kaon

$$i\, p^\mu\, f_K\, \delta_{ab} = -\, g_K \int \frac{d^4k}{(2\pi)^4} \times \mathrm{Tr}\left[\tfrac{1}{2}\gamma^\mu\, \gamma_5\, \lambda_a\, S(k+p)\gamma_5\, \lambda_b\, S(k)\right], \tag{16}$$

where $a, b = 4, 5, 6, 7$; the trace is over Dirac, color and flavor space; and the quark propagator is given by Eq. (7). Therefore

$$f_K = -12i\, g_K \int \frac{d^4k}{(2\pi)^4} \frac{M_s + \frac{p\cdot k}{p^2}(M_s - M)}{[(p+k)^2 - M_s^2][k^2 - M^2]}. \tag{17}$$

Introducing Feynman parameters gives

$$f_K = -12i\, g_K \int_0^1 dx \int \frac{d^4k}{(2\pi)^4} \times \frac{M_s - x(M_s - M)}{[k^2 + x(1-x)\, m_K^2 - M_s^2 + x(M_s^2 - M^2)]^2}. \tag{18}$$

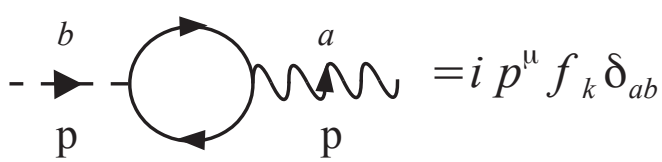

Figure 4. Diagram representing the pseudoscalar meson decay constant. The dashed line represents a pseudoscalar meson and the wavy line an external axialvector field.

By Wick rotating and introducing the proper-time regularization scheme we find

$$f_K = \frac{3\, g_K}{4\pi^2} \int_0^1 dx \int_{1/\Lambda_{UV}^2}^{1/\Lambda_{IR}^2} d\tau\, \frac{1}{\tau}\, \left[M_s + x\,(M - M_s)\right] \times e^{-\tau[M_s^2 - x(M_s^2 - M^2) - x(1-x)m_K^2]}. \tag{19}$$

The result for f_π is obtained from Eq. (19) via the substitutions: $M_s \to M$, $g_K \to g_\pi$ and $m_K \to m_\pi$.

III. PION AND KAON FORM FACTORS

The electromagnetic current, $j^\mu(p', p)$, of a hadron is defined by

$$\int d^4z\, e^{-iqz} \left\langle \vec{p}\,' \left| \bar{\psi}(z)\, \tfrac{1}{2}\left(\lambda_3 + \tfrac{1}{\sqrt{3}}\lambda_8\right) \gamma^\mu\, \psi(z) \right| \vec{p} \right\rangle \equiv \sqrt{4\, E_p\, E_{p'}}\ (2\pi)^4\, \delta^{(4)}(p' - p - q)\, j^\mu(p', p), \tag{20}$$

where $E_p = \sqrt{\vec{p}^{\,2} + m_k^2}$, $q = p' - p$ and the normalization of state vectors is

$$\langle \vec{p}\,'|\vec{p}\rangle = 2\,(2\pi)^3\, E_p\, \delta^{(3)}(\vec{p}\,' - \vec{p}). \tag{21}$$

For the case of a pseudoscalar meson, the electromagnetic current is parameterized by a single form factor and takes the form

$$\sqrt{4\, E_p\, E_{p'}}\ j_k^\mu(p', p) \equiv (p'^\mu + p^\mu)\, F_k(Q^2), \tag{22}$$

where $Q^2 \equiv -q^2$.

In the NJL model considered here the pion and kaon electromagnetic current is given by the two diagrams of Fig. 5; and in this section we determine the pion and kaon form factors at three levels of sophistication. Firstly the pseudoscalar form factors are obtained by treating the dressed quarks like point (bare) particles; in the second case a pion loop on the dressed quarks is included; and finally at the third level of sophistication we also include vector meson contributions to the quark-photon vertex.

A. Pion and Kaon form factors: bare quarks

The coupling of a photon to a point-like (bare) quark is given by

$$\Lambda_q^{\mu,(\mathrm{bare})} = \frac{1}{2}\left(\lambda_3 + \frac{1}{\sqrt{3}}\lambda_8\right)\gamma^\mu = \begin{pmatrix} \frac{1}{6} + \frac{\tau_3}{2} & 0 \\ 0 & e_s \end{pmatrix} \gamma^\mu, \tag{23}$$

where τ_3 is a Pauli matrix and e_s is the s quark charge. With the quark-photon vertex given by Eq. (23) the electromagnetic current of the π^+, obtained from the diagrams in Fig. 5, reads

$$j_\pi^{\mu,(\mathrm{bare})}(p', p) = j_{\pi,1}^{\mu,(\mathrm{bare})}(p', p) + j_{\pi,2}^{\mu,(\mathrm{bare})}(p', p), \tag{24}$$

---

contributions are proportional to p^2 and therefore expected to be small near the pion pole. The mixing contributions to the pion form factor, however, may become important for high values of Q^2.

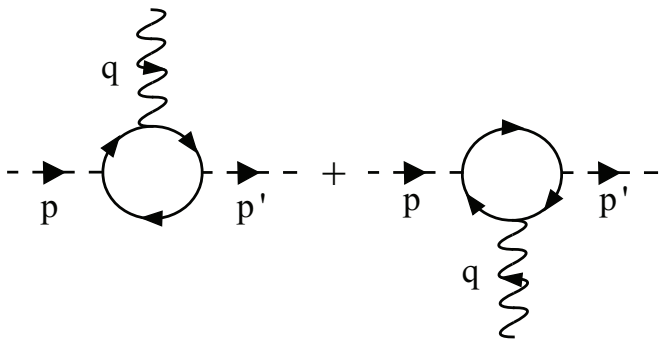

Figure 5. Feynman diagrams for the meson electromagnetic current.

where

$$j^{\mu,(\mathrm{bare})}_{\pi,1}(p',p) = \frac{i\,g_\pi^2}{\sqrt{4\,E_p\,E_{p'}}}\int\frac{d^4k}{(2\pi)^4}$$
$$\mathrm{Tr}\left[\gamma_5\,\tau_-\,S(k+p')\,\Lambda_q^{\mu,(\mathrm{bare})}\,S(k+p)\,\gamma_5\,\tau_+\,S(k)\right], \quad (25)$$
$$j^{\mu,(\mathrm{bare})}_{\pi,2}(p',p) = \frac{i\,g_\pi^2}{\sqrt{4\,E_p\,E_{p'}}}\int\frac{d^4k}{(2\pi)^4}$$
$$\mathrm{Tr}\left[\gamma_5\,\tau_+\,S(k-p)\,\Lambda_q^{\mu,(\mathrm{bare})}\,S(k-p')\,\gamma_5\,\tau_-\,S(k)\right]. \quad (26)$$

Note, the first term of the current corresponds to the left diagram in Fig. 5 and $j^{\mu,(\mathrm{bare})}_{\pi,2}$ the right diagram. The flavor matrices from the Bethe-Salpeter vertices in Eqs. (25)–(26) are defined as $\tau_\pm \equiv \frac{1}{\sqrt{2}}(\lambda_1 \pm i\lambda_2)$ and the quark propagator is given by Eq. (7).[5] The K^+ electromagnetic current reads

$$j^{\mu,(\mathrm{bare})}_K(p',p) = j^{\mu,(\mathrm{bare})}_{K,1}(p',p) + j^{\mu,(\mathrm{bare})}_{K,2}(p',p), \quad (27)$$

where $j^{\mu,(\mathrm{bare})}_{K,1}$ and $j^{\mu,(\mathrm{bare})}_{K,2}$ are obtained from Eqs. (25) and (26), respectively, via the substitutions $g_\pi \to g_K$ and $\tau_\pm \to \lambda_\pm \equiv \frac{1}{\sqrt{2}}(\lambda_4 \pm i\lambda_5)$.

Taking the trace and introducing Feynman parameters, the (bare) pion and kaon form factors are given by

$$F_\pi^{(\mathrm{bare})}(Q^2) = 24i\,g_\pi^2\int\frac{d^4k}{(2\pi)^4}\int_0^1 dx$$
$$\times\left[\frac{-x}{[k^2-\triangle_1]^2} + \frac{1}{2}\,m_\pi^2\int_{-x}^{x}dy\,\frac{x}{[k^2-\triangle_2]^3}\right], \quad (28)$$

[5] For the π^+, with $M_u = M_d$, the two pieces of the current are related by $e_u^{-1}\,j^\mu_{\pi,1} = -e_d^{-1}\,j^\mu_{\pi,2}$ and could therefore be written as a single term.

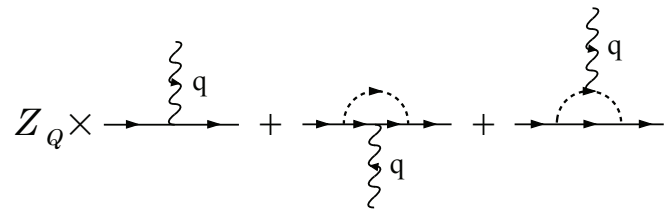

Figure 6. Feynman diagrams for the quark electromagnetic current with a pion cloud.

$$F_K^{(\mathrm{bare})}(Q^2) = 8i\,g_K^2\int\frac{d^4k}{(2\pi)^4}\int_0^1 dx$$
$$\times\left\{\frac{-2x}{[k^2-\triangle_1]^2} + \frac{-x}{[k^2-\triangle_3]^2}\right.$$
$$\left. + \int_{-x}^{x}dy\left[\frac{2N_1}{[k^2-\triangle_4]^3} + \frac{N_2}{[k^2-\triangle_5]^3}\right]\right\}, \quad (29)$$

with

$$\triangle_1 = M^2 + x(1-x)\,Q^2, \quad (30)$$
$$\triangle_2 = M^2 - x(1-x)\,m_\pi^2 + \frac{1}{4}Q^2(x^2-y^2), \quad (31)$$
$$\triangle_3 = M_s^2 + x(1-x)\,Q^2, \quad (32)$$
$$\triangle_4 = x\,M^2 + (1-x)\left(M_s^2 - x\,m_K^2\right) + \frac{Q^2}{4}(x^2-y^2), \quad (33)$$
$$\triangle_5 = x\,M_s^2 + (1-x)\left(M^2 - x\,m_K^2\right) + \frac{Q^2}{4}(x^2-y^2), \quad (34)$$

and

$$N_1 = (1-x)\,MM_s - M_s^2 + \frac{x}{2}\left(M^2 + M_s^2 + m_K^2\right), \quad (35)$$
$$N_2 = (1-x)\,MM_s - M^2 + \frac{x}{2}\left(M^2 + M_s^2 + m_K^2\right). \quad (36)$$

In the limit where $M = M_s$, and therefore $m_\pi = m_K$ and $g_\pi = g_K$, the pion and kaon from factors are identical.

B. Pion and Kaon form factors: pion cloud

In the previous subsection, we treated the coupling of the photon to the dressed quarks as point-like. In general, however, the constituent quarks are dressed by a cloud of mesons. Because the pion is the lightest meson, effects of the pion cloud can contribute significantly to meson form factors for $Q^2 \lesssim 1\,\mathrm{GeV}^2$ [31]. Because of isospin conservation the s-quark cannot be dressed by the pion cloud and therefore the pion cloud contribution to the pion form factor will be about twice that for the kaon form factor. In this subsection we consider corrections to the quark-photon vertex from pion loops around a constituent quark, as illustrated in Fig. 6, and determine their contribution to pion and kaon form factors.

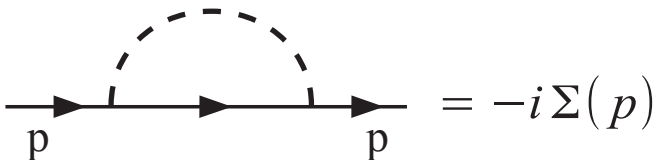

Figure 7. Pion cloud self-energy diagram for the light quarks.

As we mentioned already in Sect. I, a full treatment of meson cloud effects is very complicated and beyond the scope of this work. Here we will follow the procedure explained in Ref. [30, 51], which has been used implicitly in many previous works and which we summarize in App. C, to incorporate a part of pion cloud effects into a renormalization of the mass and wave function of the light dressed quarks. [6] Only for the quantity which is of most interest to our present work, namely the electromagnetic quark-photon vertex, the pion cloud effects are resolved and explicitly treated.

Including pion loop corrections modifies the flavor $SU(2)$ piece of Eq. (23), such that[7]

$$\left(\frac{1}{6}+\frac{\tau_3}{2}\right)\gamma^\mu \longrightarrow\; Z_Q\left(\frac{1}{6}+\frac{\tau_3}{2}\right)\gamma^\mu + \frac{1}{2}\,(1-\tau_3)\,\Lambda^\mu_Q(p',p)+\tau_3\,\Lambda^\mu_\pi(p',p), \quad (37)$$

where each term is associated with the corresponding diagram in Fig. 6. The quark wave function renormalization, Z_Q, is essential for charge conservation and is interpreted as the probability of striking a dressed quark without its pion cloud. It is given by (see App. C)

$$Z_Q = 1 + \left.\frac{\partial\Sigma(p)}{\partial\not{p}}\right|_{\not{p}=M}, \quad (38)$$

where $\Sigma(p)$ is the light quark self-energy arising from the pion cloud, illustrated in Fig. 7. This self-energy reads

$$\Sigma(p) = 3i\,g_\pi^2\int\frac{d^4k}{(2\pi)^4}\;iD_\pi(p-k)\,\gamma_5\,iS_\ell(k)\,\gamma_5, \quad (39)$$

where $D_\pi(p)$ denotes the pion propagator given by

$$D_\pi(p) = \frac{1}{p^2-m_\pi^2+i\varepsilon}. \quad (40)$$

[6] In App. C, we also discuss the validity of low-energy theorems relevant in the present context, like the Goldberger-Treiman (GT) relation [52] or the Gell-Mann - Oakes - Renner (GOR) relation[53].

[7] Contributions from a kaon cloud would modify each piece of Eq. (23).

The vertex functions of Eq. (37) take the form

$$\Lambda^\mu_Q(p',p) = g_\pi^2\int\frac{d^4k}{(2\pi)^4}\;\gamma_5\,iS_\ell(p'-k)\,\gamma^\mu\,iS_\ell(p-k)\,\gamma_5\,iD_\pi(k), \quad (41)$$

$$\Lambda^\mu_\pi(p',p) = 2\,g_\pi^2\;(p'^\mu+p^\mu)\,F_\pi^{(\mathrm{bare})}(q^2)\int\frac{d^4k}{(2\pi)^4}\;iD_\pi(p'-k)\,iD_\pi(p-k)\,\gamma_5\,iS(k)\,\gamma_5, \quad (42)$$

where p' and p are the external momenta of the quarks. The off-shell vertex functions of Eqs. (41)–(42) are approximated by their on-shell form in our calculation of the meson form factors. The vertex functions in Eq. (37) can therefore be expressed in the form

$$\Lambda^\mu_Q(p',p) = \gamma^\mu F_{1Q}^{(q)}(Q^2)+\frac{i\sigma^{\mu\nu}q_\nu}{2M}F_{2Q}^{(q)}(Q^2), \quad (43)$$

$$\Lambda^\mu_\pi(p',p) = \gamma^\mu F_{1Q}^{(\pi)}(Q^2)+\frac{i\sigma^{\mu\nu}q_\nu}{2M}F_{2Q}^{(\pi)}(Q^2). \quad (44)$$

Expressions for these dressed quark form factors are given in App. D. The flavor $SU(2)$ piece of the quark-photon vertex (see Eq. (23)) including pion loop effects therefore reads

$$\Lambda^{\mu,(\pi)}_{SU(2)}(q) = Z_Q\left(\frac{1}{6}+\frac{\tau_3}{2}\right)\gamma^\mu + \gamma^\mu\left[\frac{1}{2}(1-\tau_3)\,F_{1Q}^{(q)}(Q^2)+\tau_3\,F_{1Q}^{(\pi)}(Q^2)\right] + \frac{i\sigma^{\mu\nu}q_\nu}{2M}\left[\frac{1}{2}(1-\tau_3)\,F_{2Q}^{(q)}(Q^2)+\tau_3F_{2Q}^{(\pi)}(Q^2)\right], \quad (45)$$

and the corresponding three-flavor vertex is therefore

$$\Lambda^{\mu,(\pi)}_Q(q) = \mathrm{diag}\left[\Lambda^{\mu,(\pi)}_{SU(2)}(q),\;e_s\,\gamma^\mu\right]. \quad (46)$$

The π^+ electromagnetic current, including the effects from the pion cloud, is therefore given by Eqs. (25)–(26) with the substitution $\Lambda_q^{\mu,(\mathrm{bare})}\to\Lambda_Q^{\mu,(\pi)}(q)$. The K^+ electromagnetic current, at the same level of sophistication, is obtained via the additional substitution $g_\pi\,\tau_\pm\to g_K\,\lambda_\pm$ in Eqs. (25)–(26).

C. Pion and Kaon form factors: vector mesons

The quark-photon vertex receives contributions from the $\bar{q}q$ T-matrix in the vector channel, as illustrated in Fig. 8; these contributions are analogous to the familiar vector meson dominance (VMD) model [54]. Because of the flavor structure of Eq. (1) the electromagnetic current of the light quarks only receives contributions from ρ^0 and ω mesons, while only the ϕ meson couples to the s quark. In this work we will not include the VMD contribution to the quark-photon vertex of the s quark because of the larger mass of the ϕ meson.

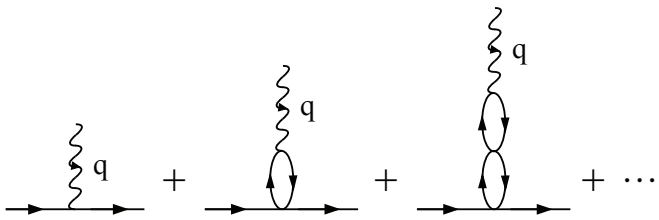

Figure 8. Dressing of the quark electromagnetic current from vector mesons.

This is consistent with our earlier approximations of neglecting the contributions of the kaon cloud and the mixing between the pseudoscalar (π) and pseudovector (a_1) meson channels.

Using the transverse Lorentz structure of the bubble diagrams in the vector $\bar{q}q$ channels, the $SU(2)$ piece of the quark-photon vertex becomes

$$\left(\frac{1}{6}+\frac{\tau_3}{2}\right)\gamma^\mu \rightarrow \left(\frac{1}{6}+\frac{\tau_3}{2}\right)\left[\gamma^\mu - \frac{2\,G_v\,\Pi_v(q^2)}{1+2\,G_v\,\Pi_v(q^2)}\left(\gamma^\mu - \frac{\not{q}q^\mu}{q^2}\right)\right], \tag{47}$$

where $\Pi_v(q^2)$ is the reduced bubble diagram in the ρ or ω channel. In the on-shell approximation for the external quark momenta the $\not{q}q^\mu$ term in Eq. (47) does not contribute to the form factors. Therefore, the VMD modification of u and d quark-photon vertices is given by

$$\gamma^\mu\left(\frac{1}{6}+\frac{\tau_3}{2}\right) \rightarrow \gamma^\mu\left(\frac{1}{6}+\frac{\tau_3}{2}\right)\frac{1}{1+2G_v\Pi_v(q^2)}. \tag{48}$$

The quark-photon vertex, including both pion cloud and vector meson effects, is therefore given by

$$\Lambda^\mu_Q(q) = \mathrm{diag}\left[\Lambda^{\mu,(\pi)}_{SU(2)}(q)\,\frac{1}{1+2G_v\Pi_v(q^2)},\; e_s\,\gamma^\mu\right]. \tag{49}$$

VMD effects on the pion form factor can simply be obtained by multiplying the entire form factor by $\left[1+2\,G_v\,\Pi_v(q^2)\right]^{-1}$. For the K^+ electromagnetic current only to the first term of Eq. (27) is multiplied by this factor, because the s quark does not couple to the ω meson. The form of $\Pi_v(q^2)$ is:

$$\Pi_v(q^2) = 48i\,q^2\int\frac{d^4k}{(2\pi)^4} \times\int_0^1 dx\,\frac{x(1-x)}{[k^2-M^2+x(1-x)q^2]^2}. \tag{50}$$

IV. RESULTS

The NJL model described here depends on two regularization parameters Λ_{UV} and Λ_{IR}; the coupling constants G_π and G_v; and the light (M) and strange (M_s) dressed quark masses.

The infrared cut-off simulates one important aspect of confinement and should therefore be similar to $\Lambda_{\rm QCD}$, we choose $\Lambda_{IR} = 0.2\,$GeV.

The coupling G_π and Λ_{UV} are fixed by the physical pion mass ($m_\pi = 0.140\,$GeV) and pion leptonic decay constant ($f_\pi = 0.0934\,$GeV); finally G_v and M_s are fixed by the physical ρ meson mass ($m_\omega \simeq m_\rho = 0.776\,$GeV) and physical kaon mass ($m_K = 0.494\,$GeV). This, therefore leaves one free parameter, the dressed light quark mass M, and in this section we investigate the M dependence of the current quark masses, the kaon decay constant, and the pion and kaon form factors.

A. Quarks masses and kaon decay constant

Results for our NJL model parameters; the light (m) and strange (m_s) current quarks masses; the kaon decay constant (f_K); the quark condensates ($\langle\bar{q}q\rangle$); together with other quantities defined in the text; are summarized in Tab. I, for values of the dressed light quark mass in the range $0.2 \leqslant M \leqslant 0.4\,$GeV. Empirical analyses of the strange to light current quark mass ratio and kaon to pion leptonic decay constant ratio have found $m_s/m = 27.5 \pm 1.0$ [32] and $f_K/f_\pi = 1.197 \pm 0.002 \pm 0.006 \pm 0.001$ [32, 33], respectively, and a recent QCD analysis [38] found $\langle\bar{s}s\rangle\,/\,\langle\bar{\ell}\ell\rangle = 1.08 \pm 0.16$ for the ratio of strange to light ($\ell = u, d$) nonperturbative (physical) quark condensates.

From an inspection of our results presented in Tab. I it is clear that good agreement with empirical values for the f_K/f_π and m_s/m ratios, and with the QCD analysis for the ratio $\langle\bar{s}s\rangle\,/\,\langle\bar{\ell}\ell\rangle$, is obtained if the dressed light quark mass has a value near $M \sim 0.25\,$GeV. Therefore, our results favor values for M which are considerably lighter than typical values used in effective quark models, like the NJL model, where $M \sim 0.4\,$GeV is the norm.

B. Pion and Kaon form factors

Results for the pion form factor are presented in Fig. 9 for our favored value of the dressed light quark mass, namely $M = 0.25\,$GeV, and in Fig. 10 pion form factor results with $M = 0.40\,$GeV are illustrated. In each figure the dotted line denotes the pion form factor result where the quark-photon vertex is treated as point-like (bare); the dash-dotted line includes effects from the pion cloud; and the dashed line is the full result which also includes vector mesons in the quark-photon vertex. The solid line shows the empirical monopole function

$$F_\pi^{(\rm emp)}(Q^2) = \frac{1}{1+Q^2/0.517\,{\rm GeV}^2}, \tag{51}$$

which is constrained to reproduce the central value of the empirical pion charge radius $\langle r_\pi\rangle = 0.672 \pm 0.008\,$fm [32].

M	Λ_{UV}	G_π	G_v	M_s	m	m_s	m_s/m	f_K	f_K/f_π	$\langle\bar{\ell}\ell\rangle$	$\langle\bar{s}s\rangle$	$\langle\bar{s}s\rangle/\langle\bar{\ell}\ell\rangle$
0.20	1.24	2.36	2.08	0.467	0.0041	0.131	31.9	0.128	1.37	$-(0.275)^3$	$-(0.329)^3$	1.71
0.25	0.84	6.12	3.06	0.502	0.0086	0.227	26.5	0.110	1.18	$-(0.214)^3$	$-(0.224)^3$	1.15
0.30	0.71	10.6	4.52	0.540	0.0123	0.293	23.8	0.010	1.07	$-(0.190)^3$	$-(0.180)^3$	0.85
0.35	0.66	15.0	6.64	0.573	0.0150	0.331	22.1	0.094	1.01	$-(0.177)^3$	$-(0.159)^3$	0.72
0.40	0.64	19.3	9.60	0.609	0.0168	0.357	21.3	0.091	0.97	$-(0.170)^3$	$-(0.148)^3$	0.70

Table I. Results for the NJL model parameters: Λ_{UV}, G_π, G_v and M_s; together with resulting values for the current quark masses, kaon decay constant, and quark condensates, all for various values of the dressed light quark mass M. Masses, decay constant and regularization parameters are in units of GeV, the Lagrangian couplings, G_π and G_v, are in units of GeV^{-2}, and quark condensates are in units of GeV^3.

From Fig. 10 it is clear that the pion form factor with $M = 0.4\,\text{GeV}$ is too soft, while the pion form factor result with $M = 0.25\,\text{GeV}$ agrees very well with the empirical result of Eq. (51).

It is interesting to note that the quark core contributions are rather similar for the $M = 0.25\,\text{GeV}$ and $M = 0.4\,\text{GeV}$ cases; and the main difference comes from the pion cloud contributions. This is understood by noting that the coupling constant g_π increases as M becomes larger (see Tab. II) – which is consistent with the flavor $SU(2)$ quark-level Goldberger-Treiman relation: $M = g_\pi f_\pi$ [19] – and therefore leads to larger effects from the pion cloud. In addition, as shown in Tab. II, the value of Z_Q – which represents the probability to find a quark without its pion cloud – decreases with increasing M, leading to larger pion cloud effects as M increases and to a smaller value of the pion form factor at high Q^2, because the quark vertex function approaches $Z_Q\, e_q\, \gamma^\mu$ as $Q^2 \to \infty$ (see Eq. (45)). The end result is that if both the pion cloud and VMD effects are added to the quark core contributions, then the data and the empirical monopole function can be reproduced very well for the case $M = 0.25\,\text{GeV}$, while for the case with $M = 0.4\,\text{GeV}$ the calculated form factor is too soft.

Figures 11 and 12 present kaon form factor results for the cases $M = 0.25\,\text{GeV}$ and $M = 0.4\,\text{GeV}$, respectively. In each figure the dotted line denotes the kaon form factor result where the quark-photon vertex is treated as point-like (bare); the dash-dotted line includes effects from the pion cloud on the light quark; and the dashed line is the full result which also includes vector mesons in the coupling of the photon to the light quark. The kaon form factor is poorly known experimentally, however in Figs. 11 and 12 the solid line represents the monopole function:

$$F_K^{(\text{emp})}(Q^2) = \frac{1}{1 + Q^2/0.744\,\text{GeV}^2}, \tag{52}$$

which is constrained to reproduce the central value of the empirical kaon charge radius $\langle r_K\rangle = 0.560 \pm 0.031\,\text{fm}$ [32]. The s quark does not couple to the pions or – under the assumptions used here – vector mesons, therefore, unlike the pion the kaon form factor is not as sensitive to corrections from the pion cloud and vector mesons. However, from Figs. 11 and 12 it is clear that our kaon form factor results have better agreement with the empirical result of Eq. (52) when $M = 0.25\,\text{GeV}$, as opposed to the case when $M = 0.4\,\text{GeV}$.

In Fig. 13 we present results for the kaon to pion form factor ratio, $F_K(Q^2)/F_\pi(Q^2)$, for the case of $M = 0.25\,\text{GeV}$. We find that this ratio, including effects from the pion cloud and vector mesons, approaches $F_K/F_\pi \sim 1.4$ as $Q^2 \to \infty$. Perturbative QCD predicts that the ratio F_K/F_π should approach f_K^2/f_π^2 as $Q^2 \to \infty$ [10, 11]. Since our calculation for $M = 0.25$ GeV reproduces the experimental values for both decay constants with the squared ratio $f_K^2/f_\pi^2 = 1.4$ (see Tab. I), we can say that our NJL model result for $M = 0.25\,\text{GeV}$ is consistent with the prediction based on perturbative QCD. This agreement cannot be attained for the case of $M = 0.4\,\text{GeV}$, where our calculated ratio of form factors becomes larger than the calculated ratio of decay constants.

However, before drawing firm conclusions about the behavior of the form factors for large values of Q^2, one should take into account the contributions of the mixing between the pseudoscalar (π) and pseudovector (a_1) meson channels, as mentioned at the end of Sect. II B.

M [GeV]	g_π	g_K	Z_Q
0.20	2.10	2.20	0.87
0.25	2.62	2.79	0.85
0.30	3.15	3.40	0.84
0.35	3.67	3.97	0.82
0.40	4.20	4.55	0.80

Table II. Results for the effective quark-meson coupling constants and the quark wave function renormalization, for various values of the dressed light quark mass M.

C. Pion and kaon charge radii

The charge radius, $\langle r_k\rangle$, of the pion and kaon is obtained from the corresponding form factor via the relation:

$$\langle r_k\rangle = \sqrt{-6\frac{\partial F_k(Q^2)}{\partial Q^2}\bigg|_{Q^2=0}}. \tag{53}$$

M	$\langle r_\pi \rangle^{(\mathrm{bare})}$	$\langle r_K \rangle^{(\mathrm{bare})}$	$\langle r_\pi \rangle^{(\mathrm{bare})} / \langle r_K \rangle^{(\mathrm{bare})}$	$\langle r_\pi \rangle^{(\pi)}$	$\langle r_K \rangle^{(\pi)}$	$\langle r_\pi \rangle^{(\pi)} / \langle r_K \rangle^{(\pi)}$	$\langle r_\pi \rangle$	$\langle r_K \rangle$	$\langle r_\pi \rangle / \langle r_K \rangle$
0.20	0.455	0.430	1.06	0.527	0.481	1.09	0.645	0.571	1.13
0.25	0.489	0.465	1.05	0.589	0.530	1.11	0.690	0.608	1.14
0.30	0.497	0.474	1.05	0.627	0.553	1.13	0.724	0.630	1.15
0.35	0.488	0.468	1.04	0.649	0.562	1.15	0.750	0.643	1.17
0.40	0.472	0.453	1.04	0.663	0.563	1.18	0.773	0.653	1.18

Table III. Pion and kaon charge radii (in units of fm) and their ratios for various choices of the dressed light quark mass (in GeV). The case labeled by (bare) corresponds to dressed quarks treated as point-like (see Eq. (23)); the case labeled by (π) corresponds to including pion cloud effects (see Eq. (46)); and the case with no superscript corresponds to including effects from both the pion cloud and vector mesons (see Eq. (49)). The values for the NJL model parameters needed to obtain these results are given in Tab. I.

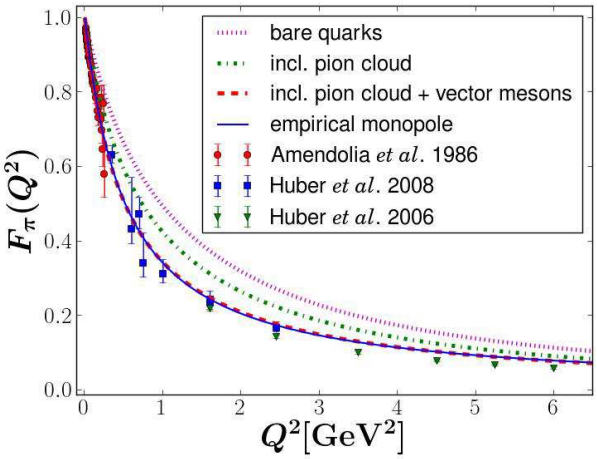

Figure 9. (Color online) Pion form factor with $M = 0.25\,\mathrm{GeV}$ (see Tab. I). The data show the experimental values from Amendolia *et al.* 1986: [6], Huber *et al.* 2008: [7] and projected values from Huber *et al.* 2006: [8].

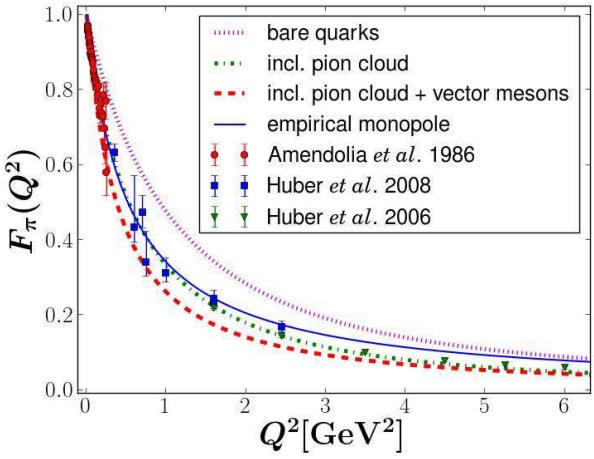

Figure 10. (Color online) Pion form factor with $M = 0.4\,\mathrm{GeV}$ (see Tab. I). The data show the experimental values from Amendolia *et al.* 1986: [6], Huber *et al.* 2008: [7] and projected values from Huber *et al.* 2006: [8].

Our results are given in Tab. III for the three variations of the photon coupling to the dressed quarks. For the case where the quark-photon vertex is treated as point-like (bare), the charge radii of the pion and kaon (including their ratios) do not depend strongly on the dressed u and d quark mass. Ref. [32] gives empirical values for the pion and kaon charge radii of: $\langle r_\pi \rangle = 0.672 \pm 0.008\,\mathrm{fm}$ and $\langle r_K \rangle = 0.560 \pm 0.031\,\mathrm{fm}$, with the ratio therefore equal to $\langle r_\pi \rangle / \langle r_K \rangle = 1.20 \pm 0.08$. For the bare quark-photon coupling we therefore find that the pion and kaon charge radii, together with their ratio, are too small.

Results for the pion and kaon charge radii, including effects form the pion cloud around the dressed quarks, are presented in the third sector of Tab. III. The pion cloud leads to a considerable enhancement of the pion charge radius, and a less pronounced enhancement of the kaon charge radius, bringing all results into better agreement with the empirical values. As discussed earlier, increasing the dressed quark mass M, results in larger values for g_π and smaller values for Z_Q (see Tab. III), and both of these effects increase the pion cloud effects for the charge radii and form factors.

Results for pion and kaon charge radii which include effects from vector mesons and the pion cloud are presented in the final sector of Tab. III. Good agreement with the empirical results is obtained when the dressed light quark mass is in the range $0.2 \leqslant M \leqslant 0.25\,\mathrm{GeV}$; while for large dressed u and d quark masses the charge radii are too large.

Within our present model description, we have therefore found that the electromagnetic properties of the pion and kaon, that is, their charge radii and the Q^2 dependence of their form factors (see Sect. IV B), are described very well if $M = 0.25\,\mathrm{GeV}$.

This is consistent with the observations discussed in Sect. IV A where results in good agreement with experiment and QCD based analyses are obtained for the kaon decay constant, current quark masses and quark conden-

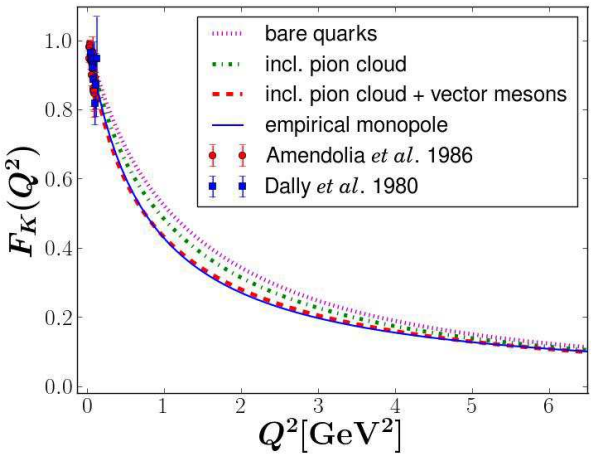

Figure 11. (Color online) Kaon form factor with $M = 0.25\,\mathrm{GeV}$ (see Tab. I). The experimental values are taken from Amendolia *et al.* 1986: [9] and Dally *et al.* 1980: [55].

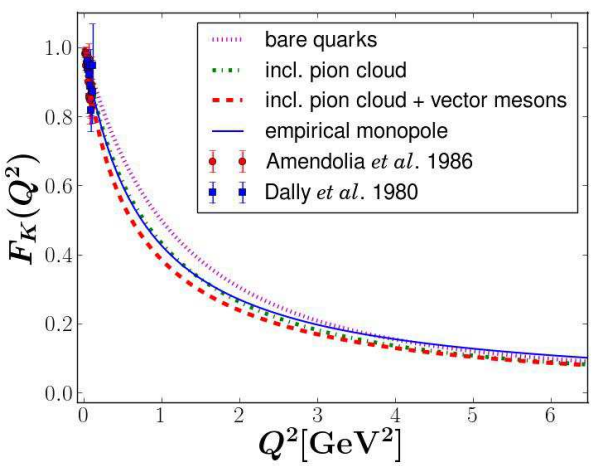

Figure 12. (Color online) Kaon form factor with $M = 0.4\,\mathrm{GeV}$ (see Tab. I). The experimental values are taken from Amendolia *et al.* 1986: [9] and Dally *et al.* 1980: [55].

sates (see Tab. I) if the dressed light quark mass is approximately $M \simeq 0.25\,\mathrm{GeV}$.

V. SUMMARY

The NJL model, including effects of the pion cloud and vector mesons at the quark level, has been used to study the pion and kaon electromagnetic form factors. An important motivation for this study was to investigate the dressed light quark (u and d) mass dependence of pion

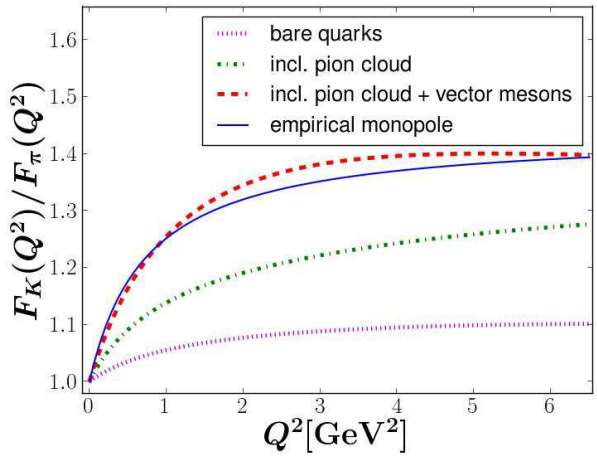

Figure 13. (Color online) Results of the ratio of the kaon form factor to the pion form factor $F_K(Q^2)/F_\pi(Q^2)$ for the case $M = 0.25$ GeV.

and kaon observables.

We began with results for the u, d, s current quark masses, quark condensates, and the kaon decay constant. Within the limits of our approximation scheme, we found that the results for the current quark mass ratio m_s/m, the ratio of condensates $\langle \bar{s}s \rangle / \langle \bar{\ell}\ell \rangle$, and the kaon decay constant are in good agreement with empirical and QCD based results if our dressed light quark mass is approximately $M \sim 0.25\,\mathrm{GeV}$.

We next studied the dressed u and d quark mass dependence of the pion and kaon form factors. We found that the pion cloud and vector mesons have a substantial effect on these form factors, and that pion cloud effects increase as the dressed light quark mass becomes larger (with fixed pion mass), as a consequence of the increased pion–quark-quark coupling. One important effect of the pion cloud is to enhance the pion charge radius more than the kaon charge radius, bringing the charge radii as well as their ratio in better agreement with empirical results.

We found that, within the limits of our approximation scheme, the available data on the form factors and charge radii are well described with relatively small values for the dressed u and d quark mass of approximately $M \sim 0.25\,\mathrm{GeV}$.

For this case, we also found that the ratio of the kaon to pion form factor for large values of Q^2 agrees very well with the perturbative QCD prediction.

Our finding that a dressed u and d quark mass of $M \sim 0.25\,\mathrm{GeV}$ leads to a good description of the pion and kaon electromagnetic properties, the kaon decay constant, and to reasonable values for the current quark masses, quark condensates and their ratios, is interesting, because so far calculations in constituent-like quark models, e.g., the NJL model or chiral soliton models [56], mostly use u and

d quark masses in the range $0.3 \lesssim M \lesssim 0.4\,\mathrm{GeV}$.

We emphasize that, because the infrared cut-off in our calculation eliminates unphysical thresholds for the decay of hadrons into quarks, there is no inherent problem with describing the heavier hadrons by using smaller dressed light quark masses.

For example, in our calculation a vector meson mass of 0.776 GeV is easily obtained, we also confirmed that a nucleon mass of 0.94 GeV can be reproduced with reasonable parameters.[8] It would be interesting to explore other hadronic properties, e.g., the nucleon electromagnetic form factors, in the domain of smaller dressed quark masses in this model description.

ACKNOWLEDGEMENTS

Y.N. wishes to thank E.V. Morooka and S. Hakamada for their careful reading of the manuscript and for their help in the preparation of some figures of the paper. W.B. acknowledges support by the Grant in Aid for Scientific Research (Kakenhi) of the Japanese Ministry of Education, Culture, Sports, Science and Technology, project no. 20168769. I.C. is supported by the Department of Energy, Office of Nuclear Physics, contract no. DE-AC02-06CH11357.

Appendix A: Regularization method

To evaluate 4-dimensional integrals, we first introduce Feynman parametrization and perform shifts of the loop momentum so that the integrand depends only on k^2, where k is the loop momentum (plus other fixed parameters). We then perform a Wick rotation and use 4-dimensional spherical coordinates to obtain

$$\int d^4k\; f(k^2) = 2\pi^2 i \int_0^\infty dk_E\, k_E^3\; f(-k_E^2), \tag{A1}$$

where $k_E = \sqrt{k_0^2 + \vec{k}^2}$ is the Euclidean length. Next, we consider the following identity:

$$\frac{1}{D^n} = \frac{1}{(n-1)!}\int_0^\infty d\tau\, \tau^{n-1}\, e^{-\tau D}, \tag{A2}$$

where D is the denominator of the integral. Here the cut-off parameters Λ_{UV} and Λ_{IR} are introduced as follows:

$$\frac{1}{(n-1)!}\int_0^\infty d\tau\; \tau^{n-1}\, e^{-\tau D} \longrightarrow \frac{1}{(n-1)!}\int_{1/\Lambda_{UV}^2}^{1/\Lambda_{IR}^2} d\tau\; \tau^{n-1}\, e^{-\tau D}. \tag{A3}$$

Only the ultraviolet cut-off parameter, Λ_{UV}, is needed to make the integrals finite, however including an infrared cut-off, Λ_{IR}, eliminates unphysical thresholds for the decay of hadrons into quarks and plays the role of simulating the confinement in the NJL model. Therefore, in the case of the loop integrals for quarks the infrared cut-off should satisfy $\Lambda_{IR} \sim \Lambda_{\mathrm{QCD}}$, however for loop integrals involving virtual pions, where these pions should not be confined, we set $\Lambda_{IR} = 0$.

Appendix B: Formulae for the bubble diagrams

In this Appendix we give formulae for the regularized bubble diagrams for the pion and kaon, which enter the pole condition equations, and the coupling constants of pion and kaon to quarks. These bubble diagrams take the form

$$\Pi_\pi(p^2) = 12i\int_0^1 dx \int \frac{d^4k}{(2\pi)^4} \times \left[\frac{p^2}{[k^2 + p^2x(1-x) - M^2]} - \frac{2}{k^2 - M^2}\right], \tag{B1}$$

$$\Pi_K(p^2) = 12i\int_0^1 dx \int \frac{d^4k}{(2\pi)^4} \times \left[\frac{p^2 - (M_s - M)^2}{[k^2 + p^2x(1-x) - x(M^2 - M_s^2) - M_s^2]} - \frac{1}{k^2 - M_s^2} - \frac{1}{k^2 - M^2}\right]. \tag{B2}$$

Introducing the cut-off parameters as explained in App. A, the regularized bubble diagrams are given by

$$\Pi_\pi(p^2) = -\frac{3}{4\pi^2}\int_0^1 dx \int_{1/\Lambda_{UV}^2}^{1/\Lambda_{IR}^2} d\tau\; \frac{1}{\tau} \times \left[\frac{2}{\tau}\, e^{-\tau M^2} + p^2\, e^{-\tau[M^2 - x(1-x)\,p^2]}\right], \tag{B3}$$

$$\Pi_K(p^2) = -\frac{3}{4\pi^2}\int_0^1 dx \int_{1/\Lambda_{UV}^2}^{1/\Lambda_{IR}^2} d\tau\; \frac{1}{\tau} \times \left[\left[p^2 - (M_s - M)^2\right] e^{-\tau[M_s^2 + x(M^2 - M_s^2) - x(1-x)\,p^2]} + \frac{1}{\tau}\left[e^{-\tau M^2} + e^{-\tau M_s^2}\right]\right]. \tag{B4}$$

[8] In the simplest quark - scalar diquark model for the nucleon, used for example in Ref. [23], one finds that for $M = 0.25\,\mathrm{GeV}$ the experimental nucleon mass can be reproduced by using $G_s/G_\pi = 0.56$, where G_s is the 4-Fermi coupling constant in the scalar quark-quark channel.

Appendix C: Renormalization of pion cloud effects

In this Appendix the standard techniques of perturbative renormalization are briefly reviewed. These techniques are applied to the renormalization of the mass, wave function normalization and charge of a dressed quark from a pion cloud (see Figs. 6 and 7), thereby giving the renormalized ("physical") values. We will restrict the discussion in this Appendix to the flavor $SU(2)$ case, because the strange quark cannot couple to the pion due to isospin conservation. Further, we will assume isospin symmetry ($m_u = m_d = m$) and refer only to the scalar and pseudoscalar interaction terms of the Lagrangian given in Eq. (1). Labeling the unrenormalized quantities with a subscript 0, and including explicitly the coupling to an external vector field V^μ, we have:

$$\mathcal{L} = \overline{\psi}_0 \left(i\partial\!\!\!/ - m_0\right) \psi_0 - \left(\overline{\psi}_0 \gamma^\mu e_0 \, \psi_0\right) V_\mu + G_{\pi 0} \left[\left(\overline{\psi}_0 \psi_0\right)^2 - \left(\overline{\psi}_0 \gamma_5 \tau_i \psi_0\right)^2 \right], \quad \text{(C1)}$$

where $\psi = (u, d)$ and e_0 is the unrenormalized flavor $SU(2)$ quark charge in units of the elementary charge. The renormalized quantities – which are the same as in the main text – are introduced by the scale transformations

$$\psi_0 = \sqrt{Z_Q}\, \psi, \quad m_0 = \frac{m}{Z_Q}, \quad G_{\pi 0} = \frac{G_\pi}{Z_Q^2}, \quad e_0 = \frac{Z_V}{Z_Q} e, \quad \text{(C2)}$$

where Z_V is the quark vertex renormalization for an external vector field, defined at zero momentum transfer. As usual, gauge invariance leads to the Ward identity result $Z_V = Z_Q$, so that the electric charge is not renormalized and given by $\left(\frac{1}{6} + \frac{\tau_3}{2}\right)$ as in Eq. (23). (Here we do not consider the renormalization of the external vector field.) After the scale transformation the Lagrangian of Eq. (C1) becomes

$$\mathcal{L} = \overline{\psi} \left(Z_Q \, i\partial\!\!\!/ - m\right) \psi - Z_V \left(\overline{\psi} \gamma^\mu e \, \psi\right) V_\mu + G_\pi \left[\left(\overline{\psi}\psi\right)^2 - \left(\overline{\psi} \tau_i \gamma_5 \psi\right)^2 \right]. \quad \text{(C3)}$$

The mass renormalization is performed in the usual manner, that is, by adding and subtracting the term $-\overline{\psi}\,(M - m)\,\psi$, where the subtracted term is treated as a counter term:

$$\mathcal{L} = \overline{\psi} \left(Z_Q \, i\partial\!\!\!/ - M\right) \psi - Z_V \left(\overline{\psi} \gamma^\mu e \, \psi\right) V_\mu + G_\pi \left[\left(\overline{\psi}\psi\right)^2 - \left(\overline{\psi} \tau_i \gamma_5 \psi\right)^2 \right] + \overline{\psi}\,(M - m)\,\psi. \quad \text{(C4)}$$

Following the standard procedure, we split $\overline{\psi}\psi$ in the second line of Eq. (C4) into an expectation value in the constituent quark vacuum, and a normal ordered product, which by definition has no vacuum expectation value. Inserting $\overline{\psi}\psi = \langle\overline{\psi}\psi\rangle + :\overline{\psi}\psi:$ into the second line of Eq. (C4), and requiring that the result becomes a "true" residual interaction without terms linear in $:\overline{\psi}\psi:$, we obtain the familiar gap equation

$$M = m - 2\, G_\pi \, \langle\overline{\psi}\psi\rangle = m + 48 i \, M \, G_\pi \int \frac{d^4k}{(2\pi)^4} \, \frac{1}{k^2 - M^2 + i\epsilon}. \quad \text{(C5)}$$

For the isospin symmetric flavor $SU(2)$ case this is the same as Eq. (3). The gap equation can therefore be viewed as a definition of normal ordering and the constituent quark vacuum. Any contribution to the mass shift, for example, from the virtual pion cloud around the dressed quark (see Fig. 7), must also be included in the counter term proportional to $(M - m)$ in Eq. (C4), which just leads to a redefinition of normal ordering and the dressed quark vacuum [45, 46]. The Lagrangian therefore becomes

$$\mathcal{L} = \overline{\psi} \left(Z_Q \, i\partial\!\!\!/ - M\right) \psi - Z_V \left(\overline{\psi} \gamma^\mu e \, \psi\right) V_\mu + G_\pi \left[\left(:\overline{\psi}\psi:\right)^2 - \left(:\overline{\psi} \gamma_5 \tau_i \psi:\right)^2 \right], \quad \text{(C6)}$$

where an irrelevant constant (c-number) term has been dropped. The quark wave function renormalization factor Z_Q is determined perturbatively from the requirement that the dressed quark propagator, including the self energy term illustrated in Fig. 7, becomes $S(p) = 1/\left(p\!\!\!/ - M + i\epsilon\right)$ as $p\!\!\!/ \to M$ [see Eq. (5)]. This gives

$$Z_Q = 1 + \left. \frac{\partial \Sigma(p)}{\partial p\!\!\!/} \right|_{p\!\!\!/ = M}, \quad \text{(C7)}$$

which is just Eq. (38). Therefore, as long as pion cloud effects are only included on the level of the mass and wave function renormalization of the dressed quark, there is no change in the standard NJL model description. To demonstrate this in more detail we verify various low-energy theorems which are important herein:

- **Goldstone theorem**: By using Eq. (C5) and the form of the bubble graph given by Eq. (B1), it is easy to verify the identity

$$\langle\overline{\psi}\psi\rangle = M \, \Pi_\pi(0), \quad \text{(C8)}$$

  which relates the quark condensate and the bubble graph $\Pi_\pi(p^2)$ at $p^2 = 0$. It then follows from the gap equation [Eq. (C5)] and the pion pole condition of Eq. (11) that $m_\pi^2 = 0$ if $m = 0$.

- **Goldberger-Treiman (GT) relation (at the quark level)**: Let us write the expression for the pion decay constant, which is obtained from Eqs. (17) and (18), by the substitutions $M_s \to M$, $g_K \to g_\pi$ and $m_K \to m_\pi$, as

$$f_\pi = g_\pi \, M \, I(p^2 = m_\pi^2), \quad \text{(C9)}$$

  where the function $I(p^2)$ is defined by

$$I(p^2) = -12 i \int \frac{d^4k}{(2\pi)^4} \frac{1}{\left[(p+k)^2 - M^2\right]\left[k^2 - M^2\right]}. \quad \text{(C10)}$$

This function is related to the bubble graph $\Pi_\pi(p^2)$ as follows [see Eq. (B1)]:

$$\Pi_\pi(p^2) - \Pi_\pi(0) = -p^2 I(p^2). \tag{C11}$$

Using the derivative of this relation w.r.t. p^2 and also Eq. (14), it follows that Eq. (C9) can be written as

$$M = g_\pi f_\pi \left(1 + C\right). \tag{C12}$$

Here C is defined as

$$C = m_\pi^2 \, \frac{I'(m_\pi^2)}{I(m_\pi^2)}, \tag{C13}$$

where the prime denotes differentiation w.r.t. p^2. Eq. (C12) is the GT relation at the quark level in the present context, where g_π and f_π are defined at the pion pole. We also note that in Eq. (C9) we assumed that the axial coupling constant of the dressed quark is given by its bare value, equal to unity. If we would use instead a model value for g_A, which may be calculated for example from the pion cloud similarly to Fig. 6, in the pion decay diagram of Fig. 4, then Eq. (C9) gets a factor g_A on the r.h.s., and the GT relation [Eq. (C12)] takes the familiar form $M\, g_A = g_\pi\, f_\pi$ in the chiral limit ($m_\pi^2 \to 0$).

- **Gell-Mann–Oakes–Renner (GOR) relation**: Note that the above relations allow us to express the gap equation and the pion pole condition in terms of the bubble graph as follows:

$$1 + 2G_\pi \Pi_\pi(0) = \frac{m}{M}, \tag{C14}$$

$$\Pi_\pi(m_\pi^2) - \Pi_\pi(0) = -m_\pi^2 I(m_\pi^2) = -\frac{m}{2G_\pi M}. \tag{C15}$$

The GOR relation is then obtained as follows:

$$\begin{aligned} -m\,\langle\overline{\psi}\psi\rangle &= \frac{M\,m}{2\,G_\pi}\left(1 - \frac{m}{M}\right) \\ &= M^2\, m_\pi^2\, I(m_\pi^2)\left(1 - \frac{m}{M}\right) \\ &= m_\pi^2\, f_\pi^2\,(1 + C)\left(1 - \frac{m}{M}\right), \end{aligned} \tag{C16}$$

where we have used Eqs. (C9) and (C12) to obtain the last line. In the chiral limit Eq. (C16) becomes the familiar GOR relation.

This concludes the verification of the low energy theorems in our present context. Finally we return to the Lagrangian of Eq. (C6) and discuss the treatment of the quark electromagnetic vertex Γ^μ, which is represented generally by Fig. 14. The "bare" vertex is given by $Z_V\, e\,\gamma^\mu = Z_Q\, e\,\gamma^\mu$ and renormalization in a "global" sense would simply mean charge renormalization, that is, according to the definition of Z_V, the replacement $\gamma^\mu \to \frac{1}{Z_V}\,\gamma^\mu$. This would give the renormalized quark vertex as $\Gamma^\mu = e\gamma^\mu$, which is correct in the limit $q \to 0$. One of the main interests of our present work, however, is to resolve this electromagnetic vertex on the level of the virtual pion cloud. For this purpose, the bare vertex $Z_Q\, e\,\gamma^\mu$, which includes the counter term from wave function renormalization, is supplemented by the corrections due to the virtual pion cloud, as shown in Fig. 6. In the pion loop diagrams (second and third diagrams of Fig. 6), we do not attempt to further resolve the pion cloud around the dressed quark. Therefore, by using $\Gamma^\mu = e\gamma^\mu$ at the quark-photon vertex in those diagrams, we obtain the expressions given in Eqs. (41) and (42). Further, inclusion of the VMD contributions (see Fig. 8) leads to the correction factor given in Eq. (48).

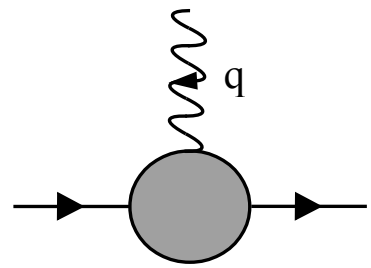

Figure 14. Graphical representation of the general quark electromagnetic vertex Γ^μ.

Appendix D: Formula for pion cloud effects

To calculate the quark wave function renormalization constant Z_Q arising from the pion cloud, we need the derivative of dressed u and d quark self-energy with respect to $\not{p}$, that is

$$\begin{aligned} \left.\frac{\partial\Sigma(p)}{\partial\not{p}}\right|_{\not{p}=M} &= \frac{3\,g_\pi^2}{8\pi^2}\int_0^1 dx \int_{1/\Lambda_{UV}^2}^\infty d\tau \\ &\times \left[x(1-x)^2 M^2 - \frac{x}{2\tau}\right] e^{-\tau[(1-x)^2 M^2 + x\, m_\pi^2]}. \end{aligned} \tag{D1}$$

In the following we give the formulae for the functions related to the quark electromagnetic vertex corrections

arising from the pion cloud:

$$F_{1Q}^{(q)}(Q^2) = \frac{g_\pi^2}{32\pi^2}\Bigg\{\int_0^1 dx \int_{1/\Lambda_{UV}^2}^\infty d\tau\, \frac{2}{\tau}\, e^{-\tau[x(1-x)Q^2+M^2]} + \int_0^1 dx \int_{-x}^x dy \int_{1/\Lambda_{UV}^2}^\infty d\tau \left[2x^2M^2 - m_\pi^2 - \frac{1}{\tau}\right] e^{-\tau A}\Bigg\}, \tag{D2}$$

$$F_{2Q}^{(q)}(Q^2) = -\frac{g_\pi^2\, M^2}{16\pi^2}\int_0^1 dx \int_{-x}^x dy \int_{1/\Lambda_{UV}^2}^\infty d\tau\; x^2\, e^{-\tau A}, \tag{D3}$$

$$F_{1Q}^{(\pi)}(Q^2) = F_\pi^{(\text{bare})}(Q^2)\,\frac{g_\pi^2}{16\pi^2} \times \int_0^1 dx \int_{-x}^x dy \int_{1/\Lambda_{UV}^2}^\infty d\tau \left[\frac{1}{\tau} - 2\,(1-x)^2\, M^2\right] e^{-\tau B}, \tag{D4}$$

$$F_{2Q}^{(\pi)}(Q^2) = F_\pi^{(\text{bare})}(Q^2)\,\frac{g_\pi^2\, M^2}{8\pi^2} \times \int_0^1 dx \int_{-x}^x dy \int_{1/\Lambda_{UV}^2}^\infty d\tau\; (1-x)^2\, e^{-\tau B}. \tag{D5}$$

where $A = (1-x)m_\pi^2 + x^2M^2 + \frac{1}{4}(x^2-y^2)\,Q^2$ and $B = x\,m_\pi^2 + (1-x)^2M^2 + \frac{1}{4}(x^2-y^2)\,Q^2$. The above expressions are used in Eq. (45) when including pion cloud contributions to the pion and kaon form factors.

The contribution of the loop calculation for the term proportional to γ^μ, in Eq. (45), to the pion form factor is simply proportional to the pion form factor with bare quark-photon coupling (see Eq. (28)). Similarly, the contribution to the kaon form factor is proportional to the sum of the first term and third term of Eqs. (29).

When using the quark-photon vertex of Eq. (45) we need to evaluate the diagrams in Fig. 5 with an operator insertion given by $i\sigma^{\mu\nu}q_\nu/2M$, which only acts on the u and d quarks. For the kaon the result is

$$\Lambda_{K,T}^\mu(p',p) = 6i\, g_K^2 \int \frac{d^4k}{(2\pi)^4} \times \text{Tr}\left[\gamma_5\,\lambda_-\, S_\ell(p'+k)\,\frac{i\sigma^{\mu\nu}q_\nu}{2M}\, S_\ell(p+k)\,\gamma_5\,\lambda_+\, S_s(k)\right] = -(p'+p)^\mu \frac{6i\, g_K^2\, Q^2}{M}\int_0^1 dx \int_{-x}^x dy \times \int \frac{d^4k}{(2\pi)^4}\,\frac{(1-x)\,M_s + x\,M}{[k^2-\triangle_4]^3}. \tag{D6}$$

Setting $M_s = M$ in Eq. (D6) gives the pion result:

$$\Lambda_{\pi,T}^\mu(p',p) = -(p'+p)^\mu\, 6i\, g_\pi^2\, Q^2 \times \int_0^1 dx \int_{-x}^x dy \int \frac{d^4k}{(2\pi)^4}\,\frac{1}{[k^2-\triangle_2]^3}. \tag{D7}$$

Therefore, the complete result for the pion form factor, including pion cloud effects, is given by

$$F_\pi(Q^2) = \left[Z_Q + F_{1Q}^{(q)}(Q^2) + F_{1Q}^{(\pi)}(Q^2)\right] F_\pi^{(\text{bare})}(Q^2) - 6i\, g_\pi^2\, Q^2\, \left[F_{2Q}^{(q)}(Q^2) + F_{2Q}^{(\pi)}(Q^2)\right] \times \int_0^1 dx \int_{-x}^x dy \int \frac{d^4k}{(2\pi)^4}\,\frac{1}{[k^2-\triangle_2]^3}. \tag{D8}$$

The final result for the kaon form factor including the pion cloud effects is:

$$F_K(Q^2) = 24i\, g_K^2\left[Z_Q + F_{1Q}^{(q)}(Q^2) + F_{1Q}^{(\pi)}(Q^2)\right] \times \int \frac{d^4k}{(2\pi)^4}\int_0^1 dx \left[\frac{-2x}{3[k^2-\triangle_1]^2} + \int_{-x}^x dy\,\frac{2N_1}{3[k^2-\triangle_4]^3}\right] - \frac{6i\, g_K^2\, Q^2}{M}\left[F_{2Q}^{(q)}(Q^2) + F_{2Q}^{(\pi)}(Q^2)\right] \times \int_0^1 dx \int_{-x}^x dy \int \frac{d^4k}{(2\pi)^4}\,\frac{(1-x)\,M_s + x\,M}{[k^2-\triangle_4]^3} + 24i\, g_K^2 \int \frac{d^4k}{(2\pi)^4}\int_0^1 dx \left[\frac{-x}{3[k^2-\triangle_3]^2} + \int_{-x}^x dy\,\frac{N_2}{3[k^2-\triangle_5]^3}\right], \tag{D9}$$

where $\triangle_1, \ldots, \triangle_5$ have been defined in Eqs. (30)–(34).

[1] A. Thomas and W. Weise, *The Structure of the Nucleon*, (Wiley-VCH, Berlin, 2001).
[2] J. Arrington, C. Roberts and J. Zanotti, J. Phys. G **34**, S23 (2007).
[3] I. C. Cloët, G. Eichmann, B. El-Bennich, T. Klahn and C. D. Roberts, Few Body Syst. **46**, 1 (2009).
[4] B. Lee, *Chiral dynamics*, (Gordon and Breach Science Publishers, New York, 1972).
[5] R. Machleidt and D. Entem, Phys. Rept. **503**, 1 (2011).
[6] S. Amendolia *et al.* [NA7 Collaboration], Nucl. Phys. B **277**, 168 (1986).
[7] G. Huber *et al.* [Jefferson Lab], Phys. Rev. C **78**, 045203 (2008).
[8] G. Huber *et al.* [Jefferson Lab], *Measurement of the Charged Pion Form Factor to High Q^2*, Jefferson Lab PAC 30 Proposal, 2006.

[9] S. Amendolia *et al.*, Phys. Lett. B **178**, 435 (1986).
[10] G. R. Farrar and D. R. Jackson, Phys. Rev. Lett. **43**, 246 (1979).
[11] G. P. Lepage and S. J. Brodsky, Phys. Rev. D **22**, 2157 (1980).
[12] R. Alkofer, A. Bender and C. D. Roberts, Int. J. Mod. Phys. A **10**, 3319 (1995).
[13] P. Maris and P. C. Tandy, Phys. Rev. C **62**, 055204 (2000).
[14] L. Chang *et al.*, Phys. Rev. Lett. **110**, 132001 (2013).
[15] A. Blin, B. Hiller and M. Schaden, Z. Phys. A **331**, 75 (1988).
[16] V. Bernard and U. G. Meißner, Phys. Rev. Lett. **61**, 2296 (1988); [Erratum-ibid. **61**, 2973 (1988)].
[17] U. Vogl and W. Weise, Prog. Part. Nucl. Phys. **27**, 195 (1991).
[18] T. Hatsuda and T. Kunihiro, Phys. Rept. **247**, 221 (1994) .
[19] S. Klevansky, Rev. Mod. Phys. **64**, 649 (1992).
[20] N. Ishii, W. Bentz and K. Yazaki, Phys. Lett. B **301**, 165 (1993).
[21] N. Ishii, W. Bentz and K. Yazaki, Phys. Lett. B **318**, 26 (1993).
[22] N. Ishii, W. Bentz and K. Yazaki, Nucl. Phys. A **587**, 617 (1995).
[23] W. Bentz and A. W. Thomas, Nucl. Phys. A **696**, 138 (2001).
[24] I. C. Cloët, W. Bentz and A. W. Thomas, Phys. Lett. B **621**, 246 (2005) .
[25] I. C. Cloët, W. Bentz and A. W. Thomas, Phys. Lett. B **659**, 214 (2008) .
[26] H. L. Roberts, L. Chang, I. C. Cloët and C. D. Roberts, Few Body Syst. **51**, 1 (2011) .
[27] J. Segovia *et al.*, Few Body Syst. **55**, 1 (2014) .
[28] D. Ebert, T. Feldmann and H. Reinhardt, Phys. Lett. B **388**, 154 (1996).
[29] G. Hellstern, R. Alkofer and H. Reinhardt, Nucl. Phys. A **625**, 697 (1997).
[30] T. Horikawa and W. Bentz, Nucl. Phys. A **762**, 102 (2005).
[31] I. C. Cloët, W. Bentz and A. W. Thomas, Phys. Rev. C **90**, 045202 (2014).
[32] J. Beringer *et al.* [Particle Data Group], Phys. Rev. D **86**, 010001 (2012).
[33] J. L. Rosner and S. Stone, arXiv:1309.1924 [hep-ex].
[34] S. Durr *et al.*, Phys. Lett. B **701**, 265 (2011).
[35] N. Carrasco *et al.*, Nucl. Phys. B **887**, (2014) 19-68 .
[36] R. Dowdall, C. Davies, G. Lepage and C. McNeile, Phys. Rev. D **88**, 074504 (2013) .
[37] A. Bazavov *et al.* [MILC Collaboration], Phys. Rev. Lett. **110**, 172003 (2013).
[38] C. McNeile *et al.*, Phys. Rev. **D87**, 034503 (2013).
[39] K. Suzuki and W. Weise, Nucl. Phys. **A 634**, 141 (1998)
[40] A. Szczurek, A. Buchmann, and A. Faessler, J. Phys. **G 22**, 1741 (1996)
[41] I. S. Towner, Phys. Rept. **155** (1987) 263
[42] A. Arima, K. Shimizu, W. Bentz, and H. Hyuga, Adv. Nucl. Phys. **18**, 1 (1987).
[43] E. N. Nikolov, W. Broniowski, C. V. Christov, G. Ripka, and K. Goeke, Nucl. Phys. **A 608**, 411 (1996)
[44] D. Dmitrašinović, H.-J. Schulze, R. Tegen, and R. H. Lemmer, Ann. Phys. **238**, 332 (1995).
[45] Y. Nambu and G. Jona-Lasinio, Phys. Rev. **122**, 345 (1961).
[46] Y. Nambu and G. Jona-Lasinio, Phys. Rev. **124**, 246 (1961).
[47] G. 't Hooft, Phys. Rev. D **14**, 3432 (1976).
[48] A. A. Osipov, B. Hiller, A. H. Blin and J. da Providencia, Annals Phys. **322**, 2021 (2007).
[49] A. Buck, R. Alkofer and H. Reinhardt, Phys. Lett. B **286**, 29 (1992).
[50] V. Bernard, U.-G. Meißner, and A. A. Osipov, Phys. Lett. **B 324**, 201 (1994).
[51] H. Mineo, W. Bentz, and K. Yazaki, Phys. Rev. **C 60**, 065201 (1999).
[52] M. Goldberger and S. Treiman, Phys. Rev. **110**, 1178 (1958).
[53] M. Gell-Mann, R. Oakes, and B. Renner, Phys. Rev. **175**, 2195 (1968).
[54] J. J. Sakurai, *Currents and Mesons*, (University of Chicago Press, Chicago, 1969).
[55] E. Dally *et al.*, Phys. Rev. Lett. **45**, 232 (1980).
[56] T. Kubota, M. Wakamatsu and T. Watabe, Phys. Rev. D **60**, 014016 (1999).